



HAL
open science

CLABAUTAIR: a new algorithm for retrieving three-dimensional cloud structure from airborne microphysical measurements

R. Scheirer, S. Schmidt

► **To cite this version:**

R. Scheirer, S. Schmidt. CLABAUTAIR: a new algorithm for retrieving three-dimensional cloud structure from airborne microphysical measurements. *Atmospheric Chemistry and Physics Discussions*, 2004, 4 (6), pp.8609-8625. hal-00304303

HAL Id: hal-00304303

<https://hal.science/hal-00304303>

Submitted on 18 Jun 2008

HAL is a multi-disciplinary open access archive for the deposit and dissemination of scientific research documents, whether they are published or not. The documents may come from teaching and research institutions in France or abroad, or from public or private research centers.

L'archive ouverte pluridisciplinaire **HAL**, est destinée au dépôt et à la diffusion de documents scientifiques de niveau recherche, publiés ou non, émanant des établissements d'enseignement et de recherche français ou étrangers, des laboratoires publics ou privés.

CLABAUTAIR: a new algorithm for retrieving three-dimensional cloud structure from airborne microphysical measurements

R. Scheirer¹ and S. Schmidt²

¹Institut für Physik der Atmosphäre, DLR, Oberpfaffenhofen, Germany

²Leibniz-Institute for Tropospheric Research, Leipzig, Germany

Received: 20 October 2004 – Accepted: 7 December 2004 – Published: 23 December 2004

Correspondence to: R. Scheirer (ronald.scheirer@dlr.de)

© 2004 Author(s). This work is licensed under a Creative Commons License.

**Retrieving cloud
structure from
airborne
measurements**

R. Scheirer and
S. Schmidt

Title Page

Abstract

Introduction

Conclusions

References

Tables

Figures

◀

▶

◀

▶

Back

Close

Full Screen / Esc

Print Version

Interactive Discussion

Abstract

A new algorithm is presented to retrieve the three-dimensional structure of clouds from airborne measurements of microphysical parameters. Data from individual flight legs are scanned for characteristic patterns, and the autocorrelation functions for several directions are used to extrapolate the observations along the flight path to a full three-dimensional distribution of the cloud field. Thereby, the mean measured profiles of microphysical parameters are imposed to the cloud field by mapping the measured probability density functions onto the model layers. The algorithm was tested by simulating flight legs through synthetic clouds (by means of Large Eddy Simulations (LES)) and applied to a stratocumulus cloud case measured during the first field experiment of the EC project INSPECTRO (INfluence of clouds on the SPECTral actinic flux in the lower TROposphere) in East Anglia, UK. The number and position of the flight tracks determine the quality of the retrieved cloud field. If they provide a representative sample of the entire field, the derived pattern closely resembles the statistical properties of the real cloud field.

1. Introduction

A challenge in three-dimensional (3-D) radiative transfer is the generation of realistic clouds as input for sophisticated radiative transfer models (e.g. Borde and Isaka, 1996; Petty, 2002). Currently, it is not possible to derive the required distribution of liquid water content and droplet sizes from observations of a single instrument. Passive satellite remote sensing instruments may provide a detailed horizontal distribution but fail to give reliable information about vertical profiles (e.g. Crewell et al., 1999). In-situ observations, on the other hand, may give data for any location but are usually restricted to only a few point measurements, e.g. along an aircraft flight track. Physical cloud-models (e.g. LES) can provide the full 3-D information of all needed microphysical properties but they do not necessarily represent real or even realistic cloud fields

Retrieving cloud structure from airborne measurements

R. Scheirer and
S. Schmidt

Title Page

Abstract

Introduction

Conclusions

References

Tables

Figures

◀

▶

◀

▶

Back

Close

Full Screen / Esc

Print Version

Interactive Discussion

(Stevens and Lenschow, 2001).

Clouds vary significantly in the three spatial dimensions and in time. Common airborne instruments sample volumes in the magnitude of a few liters during a single leg while cumulus clouds, for example, often cover a volume of around 10^9 m^3 . The major part of the clouds are thus not considered for its characterization which is a significant limitation because of the cloud's large variability (Evans et al., 2003). Therefore, aircraft measurements alone seem to be generally not sufficient to characterize the properties of inhomogeneous cloud layers.

On the other hand the spatial distribution of cloud droplets exhibit rather a patchy structure than following Poisson statistics (i.e. droplet concentrations in two adjacent volumes won't show an independent behavior), so that there should be a spatial correlation of droplet concentrations (Kostinski and Jameson, 2000). This structure is organized by entrainment and turbulence at several length scales. For micro-scale turbulence this is shown by Shaw et al. (1998). The turbulent spectrum is determined by the state of the atmosphere. For homogeneous conditions within a limited area and time period, a similar behavior of the corresponding cloud field is expected. Thus, in some cases such as for stratiform overcast or broken cloud fields, aircraft line measurements along a limited number of flight legs are representative for the whole layer under stable conditions. For example, Los and Duyenkerke (2000) and Räisänen et al. (2003) generated two-dimensional cloud fields from in-cloud aircraft measurements. However, they required some assumptions about cloud top and base structure, and about the profile of microphysical parameters.

This study introduces a new algorithm which generates 3-D cloud fields using aircraft measurements of liquid water content and effective radius without additional assumptions. In Sect. 2, the extrapolation of the 3-D structure from one-dimensional aircraft measurements, and thus the filling of the gaps is described. Subsequently, the algorithm is applied to a synthetic cloud field (Sect. 3) and to a measured cloud case (Sect. 4), and a preliminary discussion of its applicability is given.

Retrieving cloud structure from airborne measurements

R. Scheirer and
S. Schmidt

Title Page

Abstract

Introduction

Conclusions

References

Tables

Figures

◀

▶

◀

▶

Back

Close

Full Screen / Esc

Print Version

Interactive Discussion

2. Algorithm

An automated algorithm (CLOUD liquid water content and effective radius retrieval By an AUTomated use of AIRcraft measurements (CLABAUTAIR)) has been developed with the intention to generate a 3-D cloud field which reproduces the statistical properties of the microphysical aircraft measurements without introducing any additional assumptions about the cloud structure. The measurements of liquid water content (*LWC*) and effective radius (R_{eff}) are scanned, and the probability density functions “PDFs” as well as the autocorrelation functions are determined for every layer, defined by the user. The patterns which are found in the autocorrelation functions are then used to extrapolate the aircraft data to a complete 3-D field.

This method is illustrated in Fig. 1a–d. Starting with measurements in a single horizontal layer the main directions sampled by the aircraft are identified. This means, the data-points are sampled by relative angular (e.g. directions from one point to each other point) bins layer by layer, to spot long straight lines of measurements (Fig. 1a). This is necessary to avoid aliasing due to the connection of different flight legs and thus to correlate only data collected within a time interval during which the cloud can be considered constant. Next, the autocorrelation functions along these directions are calculated (Fig. 1b).

Then the measured *LWC* and R_{eff} are replaced by their anomalies (i.e. deviations from the layers mean). To extrapolate the observations, individual empty boxes are randomly selected within the 3-D space. The requested parameters ξ (anomaly of *LWC* or R_{eff}) for each of these boxes are calculated by a weighted average over the *I* filled boxes along the *J* main directions (Fig. 1c). The weighting is performed by the autocorrelation coefficient *r* valid for the distance $\delta = |\mathbf{x} - \mathbf{x}_{i,j}|$ between the center of the current (already filled) box at $(\mathbf{x}_{i,j})$ and the *i*th box under calculation for the *j*th direction

Retrieving cloud structure from airborne measurements

R. Scheirer and
S. Schmidt

Title Page

Abstract

Introduction

Conclusions

References

Tables

Figures

◀

▶

◀

▶

Back

Close

Full Screen / Esc

Print Version

Interactive Discussion

at (\mathbf{x}) (marked with a question mark in Fig. 1c):

$$\xi(\mathbf{x}) = \frac{\sum_{j=1}^J \sum_{i=1}^{I(j)} r_j(|\mathbf{x} - \mathbf{x}_{i,j}|) \xi(\mathbf{x}_{i,j})}{\sum_{j=1}^J \sum_{i=1}^{I(j)} |r_j(|\mathbf{x} - \mathbf{x}_{i,j}|)|} \quad (1)$$

If the weighting sum

$$\sum_{j=1}^J \sum_{i=1}^{I(j)} |r_j(|\mathbf{x} - \mathbf{x}_{i,j}|)| \quad (2)$$

5 fails to reach a certain threshold, calculation of $\xi(\mathbf{x})$ will be postponed. Initially¹ this threshold is set to 3 to take into account only calculations with a minimum attendance of contributing boxes. Due to the use of anomalies instead of absolute values this approach is also meaningful in case of negative autocorrelation coefficients. Adjacent boxes from the next layer above and below the chosen one (if already calculated) are
 10 taken into account with a fixed weight² of 0.95. This step is repeated until all boxes are filled. Finally, the “PDF” of the measurements (including the cloud-free parts to permit cloud fractions smaller than 1) are mapped onto the thus derived spatial distributions. This is done for all cloudy layers separately. Figure 1d shows the final cloud field.

15 The possible spatial resolution depends on the number, the direction, and the length of the flight legs, the sampling rate, and on the autocorrelation function. For the cases used in this study, horizontal resolutions between 50 m and 250 m and vertical resolutions between 50 m and 100 m were used.

¹if this threshold results in accepting less than 1% of the calculations it will be reduced temporarily.

²Actually this weight depends on the vertical resolution but for magnitudes used in this study, the stated weight is reasonable.

Retrieving cloud structure from airborne measurements

R. Scheirer and
S. Schmidt

Title Page

Abstract

Introduction

Conclusions

References

Tables

Figures

◀

▶

◀

▶

Back

Close

Full Screen / Esc

Print Version

Interactive Discussion

3. Test of the method

The algorithm was tested with a synthetic cloud field. A large eddy simulation (*LES*) of a stratocumulus field provided by the Intercomparison of 3-D Radiation Codes (I3RC, at <http://i3rc.gsfc.nasa.gov>) was chosen for this test. The *LES* cloud field has a horizontal resolution of 55 m and a vertical resolution of 25 m. With 64 times 64 boxes the domain size is $3.5 \times 3.5 \text{ km}^2$. The clouds are located between 400 m and 800 m altitude. Within this cloud field samples were taken by virtual flights. The flight starts at the center of the area at the ground with a random direction and an ascent angle of 10° . A new direction is selected by random if the border is reached. If cloud top is exceeded, the descend starts in the same manner but at a flatter angle (0.5°). Samples are taken every 10 m with a random error of $\pm 5\%$ added to the data. Typically about 2% of the total model boxes are described by virtual measurements so that about 98% had to be calculated by our algorithm.

For the retrieved cloud field, the horizontal resolution was set to 43 m and the vertical to 39 m to avoid the unrealistic case of model boxes that fit perfectly to the source cloud. Three examples of different flight patterns and the resulting retrievals are given in Fig. 2. We found that the gain in information by following the same flight-track at different altitudes is marginal (left column) because of the large vertical correlation of microphysical properties. Therefore we recommend random-like flight patterns (middle and right column) to get more independent information and to sample a larger area. Figure 3 shows the frequency of optical thicknesses for the original cloud field as well as for the retrieval-mean of 200 random flights. The original cloud-fraction is 0.926 while the retrieval-mean gives 0.959 with a standard deviation of 0.018. For the cloud volume the retrieval provides a mean of 1.860 km^3 and a standard deviation of 0.123 km^3 while the original volume is 1.874 km^3 . So we found CLABAUTAIR to reproduce the cloud fields features in a reasonable accuracy.

Retrieving cloud structure from airborne measurements

R. Scheirer and
S. Schmidt

Title Page

Abstract

Introduction

Conclusions

References

Tables

Figures

◀

▶

◀

▶

Back

Close

Full Screen / Esc

Print Version

Interactive Discussion

4. Application to field measurements

4.1. Aircraft data

The first application of the algorithm to in-situ microphysical data was performed for a cloud situation which was measured during the first field experiment of the EC project INSPECTRO (INfluence of clouds on the SPECTral actinic flux in the lower TROpo-sphere) on 14 September 2002, on the coast of East Anglia, United Kingdom. On this day, a stable stratus layer which was moving into land at a speed of about 10 m/s was observed between 500 and 1100 m altitude. The microphysical measurements used for this study were performed with a two-propeller research aircraft, a Partenavia P68B, which was equipped with meteorological, microphysical, and radiation instrumentation. The microphysical cloud properties were measured with a Fast Forward Scattering Spectrometer Probe (Fast-FSSP, Brenguier et al., 1998) and a Particle Volume Monitor (PVM-100, Gerber et al., 1994). The Fast-FSSP measures the cloud drop size distribution by detecting the forward scattering signal of each individual droplet passing a laser beam. From the drop size distribution, bulk parameters such as the LWC , the drop concentration, and R_{eff} can be derived (Schmidt, 2004). In contrast, the PVM-100A measures the LWC directly by detecting the scattering signal of an ensemble of droplets. For this study, the LWC measurements by the PVM-100A were used because of the high accuracy and temporal resolution of the data. The effective droplet radius R_{eff} was derived from the FSSP measurements because of its higher accuracy for size distributions.

In order to examine the three-dimensional cloud structure, several ascents and descents through the cloud layer were flown by the aircraft. In addition, one triangular flight pattern within the layer was performed. Figure 4 shows the two-dimensional “PDFs” of the LWC and R_{eff} for three different altitudes. They were determined by combining the measurements of the PVM-100A and the Fast-FSSP, and binning them into several height layers. The color scale in the plots corresponds to the probability of a particular LWC and R_{eff} at the respective level. These two-dimensional “PDFs” reflect

Retrieving cloud structure from airborne measurements

R. Scheirer and
S. Schmidt

Title Page

Abstract

Introduction

Conclusions

References

Tables

Figures

◀

▶

◀

▶

Back

Close

Full Screen / Esc

Print Version

Interactive Discussion

the microphysical properties accumulated throughout the cloud layer. The layer cloud fraction as a macrophysical property is also deduced from the microphysical measurements. The horizontal structure is contained in the autocorrelation functions which are calculated for the three legs of the triangle.

5 4.2. Retrieved cloud fields

For the INSPECTRO cloud case which is described in Sect. 4.1, the output of the algorithm was quantitatively compared with the measurements by analyzing the measured and retrieved profiles of the LWC and the power spectra along horizontal lines.

10 In Fig. 5, measured and reconstructed profiles of the LWC are displayed. The circles show the PVM-100A measurements. At 800 m, the horizontal flight pattern was performed. The range of LWC values measured at this altitude reflects the high variability which prevails even in a stratus layer. The solid blue line shows the mean reconstructed LWC profile. The error bars indicate the standard deviation which was found throughout the grid. It reproduces well the range of LWC values which were measured during
15 the horizontal leg. The dashed and dash-dotted blue lines correspond to the maximum and minimum LWC values, respectively, which are generated at the levels. The cloud top and base heights vary approximately within 200 m.

The horizontal structure of the measured and reconstructed cloud is compared in Fig. 6 by means of power spectra $P(k)$ where k denotes the wavenumber. The dotted
20 line with open circles shows the power spectrum which was calculated from PVM-100A measurements along one of the legs of the triangular pattern within the cloud layer (about 20 km length). The measurements are in agreement with the $k^{-5/3}$ scaling law (thin solid line) which is typically found for real clouds (Davis et al., 1996). The power spectra from the reproduced cloud were obtained by calculating power spectra over
25 horizontal lines throughout the grid and by subsequent averaging. The direction of the lines was chosen along and across the flight leg whose power spectrum is displayed. The red line shows the averaged power spectrum of lines parallel to the leg direction.

Retrieving cloud structure from airborne measurements

R. Scheirer and
S. Schmidt

Title Page

Abstract

Introduction

Conclusions

References

Tables

Figures

◀

▶

◀

▶

Back

Close

Full Screen / Esc

Print Version

Interactive Discussion

Retrieving cloud structure from airborne measurementsR. Scheirer and
S. Schmidt

[Title Page](#)[Abstract](#)[Introduction](#)[Conclusions](#)[References](#)[Tables](#)[Figures](#)[◀](#)[▶](#)[◀](#)[▶](#)[Back](#)[Close](#)[Full Screen / Esc](#)[Print Version](#)[Interactive Discussion](#)

In general the $k^{-5/3}$ scaling is well reproduced. However, the variability is slightly over-estimated by the generator for large wavenumbers. The blue line shows the averaged power spectrum from lines across the leg direction. In this case, the variability shows a better agreement with the measurements. The power spectra for the PVM-100A data measured along other legs of the in-cloud pattern are similar to the power spectrum which is displayed in Fig. 6. Thus, the differences between power spectra along different directions of the reproduced cloud field cannot be explained by the measurements. However, the power spectra of the reproduced cloud field agree with the observations within the range of measurement uncertainty.

5. Conclusions

A new algorithm for the retrieval of 3-D cloud fields based on aircraft measurements has been developed.

Testing our algorithm with a complete LES cloud field, we found a promising agreement between the original and retrieved cloud features. The retrieval mean cloud-fraction provides an error of about 3.6% and the retrieval mean cloud-volume an error of about 0.8%. For the sampling of cloud fields we recommend to follow random-like instead of flight patterns that imply similar paths at different altitudes.

From an application to real measurements we learned that within the measurement uncertainty, the characteristics of the simulated clouds agree with the observed counterparts.

It must be stated that the presented algorithm is limited to a moderate wind-speed and stable conditions, i.e. no significant change in the cloud pattern should occur during the measurements (no rapid convective growth). Rather than reproducing the original cloud situation, CLABAUTAIR supplies a cloud field whose statistical properties match the aircraft measurements. This could also be valid for the spiky behavior (the intermittency, e.g. Davis et al., 1994) of natural clouds, if found within the measurements, i.e.

if the database is really representative. Nevertheless, additional work will be done on validation and improvement of the presented algorithm.

Acknowledgements. This work was funded by the European project INSPECTRO (Influence of clouds on the spectral actinic flux in the lower troposphere), contract EVK2-2001-00135. Enviscope GmbH, Frankfurt, Germany, operated the aircraft during the experiment: Thanks to R. Maser, D. Schell, and H. Franke, and to the pilot B. Schumacher. L. Hinkelman, Langley Research Center, Hampton, USA provided us with LES cloud fields used for preliminary tests.

References

- Borde, R. and Isaka, H.: Radiative transfer in multifractal clouds, *J. Geophys. Res.*, 101(D23), 29 461–29 478, 1996.
- Brenguier, J. L., Bourriane, T., Coelho, A., Isbert, J., Peytavi, R., Trevarin, D., and Weschler, P.: Improvements of droplet size distribution measurements with the Fast-FSSP (Forward Scattering Spectrometer Probe). *J. Atmos. Oceanic Technol.*, 15, 1077–1090, 1998.
- Crewell, S., Hasse, G., Löhnert, U., Mebold, H., and Simmer, C.: A Ground Based Multi-Sensor System for the Remote Sensing of Clouds, *Phys. Chem. Earth (B)*, 24, 207–211, 1999.
- Davis, A., Marshak, A., Wiscombe, W., and Cahalan, R.: Multifractal characterizations of non-stationarity and intermittency in geophysical fields: Observed, retrieved, or simulated, *J. Geophys. Res.*, 99(D4), 8055–8072, 1994.
- Davis, A., Marshak, A., Wiscombe, W., and Cahalan, R.: Scale Invariance of Liquid Water Distributions in Marine Stratocumulus, Part I: Spectral Properties and Stationarity Issues, *J. Atmos. Sci.*, 53, 1538–1558, 1996.
- Evans, K. F., Lawson, R. P., Zmarzly, P., O'Connor, D., and Wiscombe, W. J.: In situ cloud sensing with multiple scattering lidar: Simulations and demonstration, *J. Atmos. Ocean Tech.*, 20, 1505–1522, 2003.
- Gerber, H., Ahrends, B. G., and Ackerman, A. S.: New microphysics sensor for aircraft use, *Atmos. Res.*, 31, 235–252, 1994.
- Kostinski, A. B. and Jameson, A. R.: On the Spatial Distribution of Cloud Particles, *J. Atmos. Sci.*, 57, 901–915, 2000.
- Los, A. and Duynerker, P. G.: Microphysical and radiative properties of inhomogeneous stra-

Retrieving cloud structure from airborne measurements

R. Scheirer and
S. Schmidt

Title Page

Abstract

Introduction

Conclusions

References

Tables

Figures

◀

▶

◀

▶

Back

Close

Full Screen / Esc

Print Version

Interactive Discussion

tocumulus: Observations and model simulations, Quart. J. R. Meteorol. Soc., 126, 3287–3307, 2000.

Petty, G. W.: Area-Average Solar Radiative Transfer in Three-Dimensionally Inhomogeneous Clouds: The Independently Scattering Cloudlet Model, J. Atmos. Sci., 59, 2910–2929, 2002.

5 Räsänen, P., Isaac, G. A., Barker, H. W., and Gultepe, I.: Solar radiative transfer for stratiform clouds with horizontal variations in liquid-water path and droplet effective radius, Quart. J. R. Meteorol. Soc., 129, 2135–2149, 2003.

Schmidt, S.: Influence of Cloud Inhomogeneities on Solar Spectral Radiation, PhD thesis, 105, Univ. Leipzig, Germany, Leipzig, 9 July 2004.

10 Shaw, R. A., Reade, W. C., Collins, L. R., and Verlinde, J.: Preferential concentration of cloud droplets by turbulence: Effects on the early evolution of cumulus cloud droplet spectra, J. Atmos. Sci., 55, 1965–1976, 1998.

Stevens, B. and Lenschow, D. H.: Observations, experiments and large eddy simulation, Bull. Amer. Meteor. Soc., 82, 283–294, 2001.

Retrieving cloud structure from airborne measurements

R. Scheirer and
S. Schmidt

Title Page

Abstract

Introduction

Conclusions

References

Tables

Figures

◀

▶

◀

▶

Back

Close

Full Screen / Esc

Print Version

Interactive Discussion

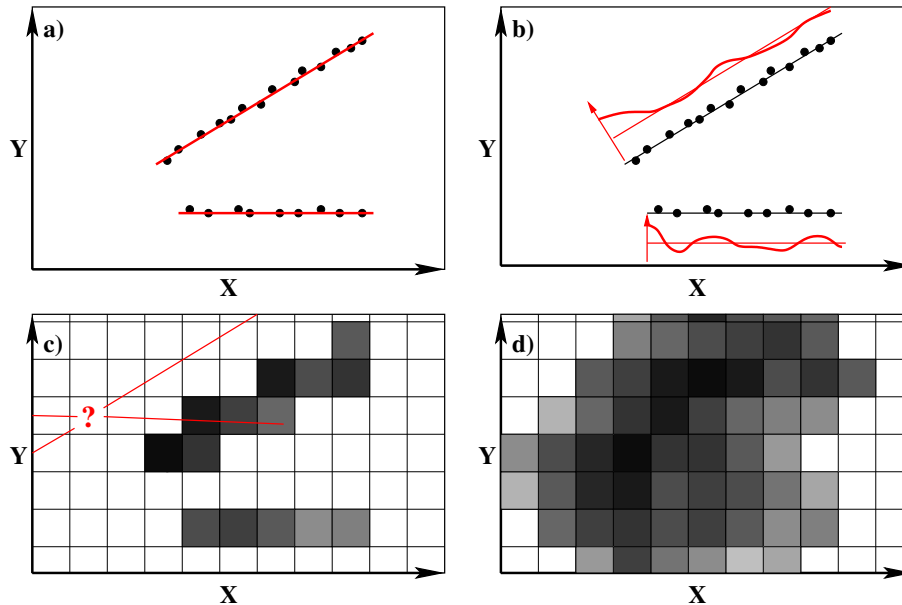
Retrieving cloud structure from airborne measurementsR. Scheirer and
S. Schmidt

Fig. 1. The four main steps of CLABAUTAIR. This figure illustrates an approach to retrieve 3-D clouds from aircraft measurements.

[Title Page](#)[Abstract](#)[Introduction](#)[Conclusions](#)[References](#)[Tables](#)[Figures](#)[◀](#)[▶](#)[◀](#)[▶](#)[Back](#)[Close](#)[Full Screen / Esc](#)[Print Version](#)[Interactive Discussion](#)

Retrieving cloud structure from airborne measurementsR. Scheirer and
S. Schmidt

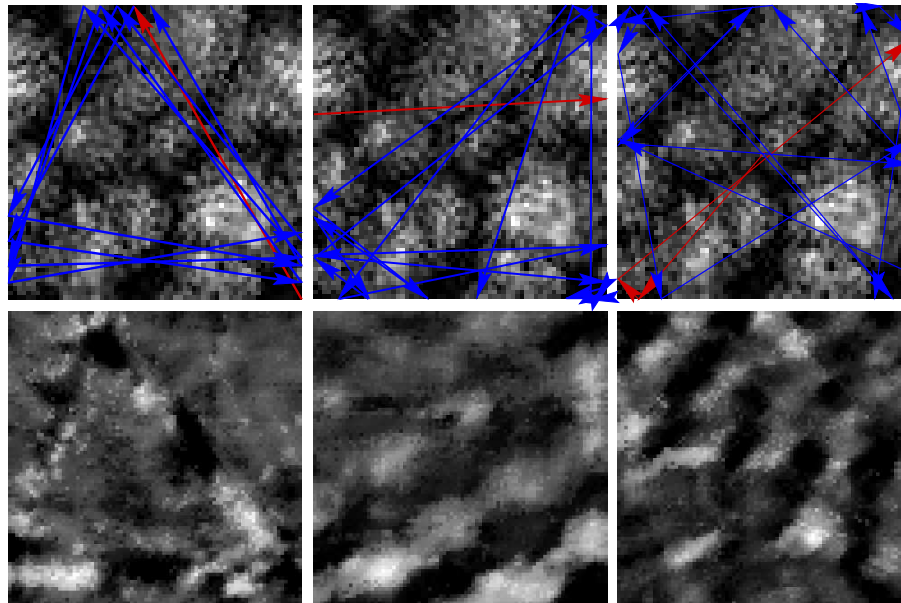


Fig. 2. Three examples of different flight patterns within a LES cloud field (upper row). Red arrows mark ascending and blue arrows descending legs. Considered are only flight legs meeting the cloudy altitudes (400 m–800 m). The retrieved cloud structures are given in the lower row.

[Title Page](#)[Abstract](#)[Introduction](#)[Conclusions](#)[References](#)[Tables](#)[Figures](#)[◀](#)[▶](#)[◀](#)[▶](#)[Back](#)[Close](#)[Full Screen / Esc](#)[Print Version](#)[Interactive Discussion](#)

Retrieving cloud structure from airborne measurementsR. Scheirer and
S. Schmidt

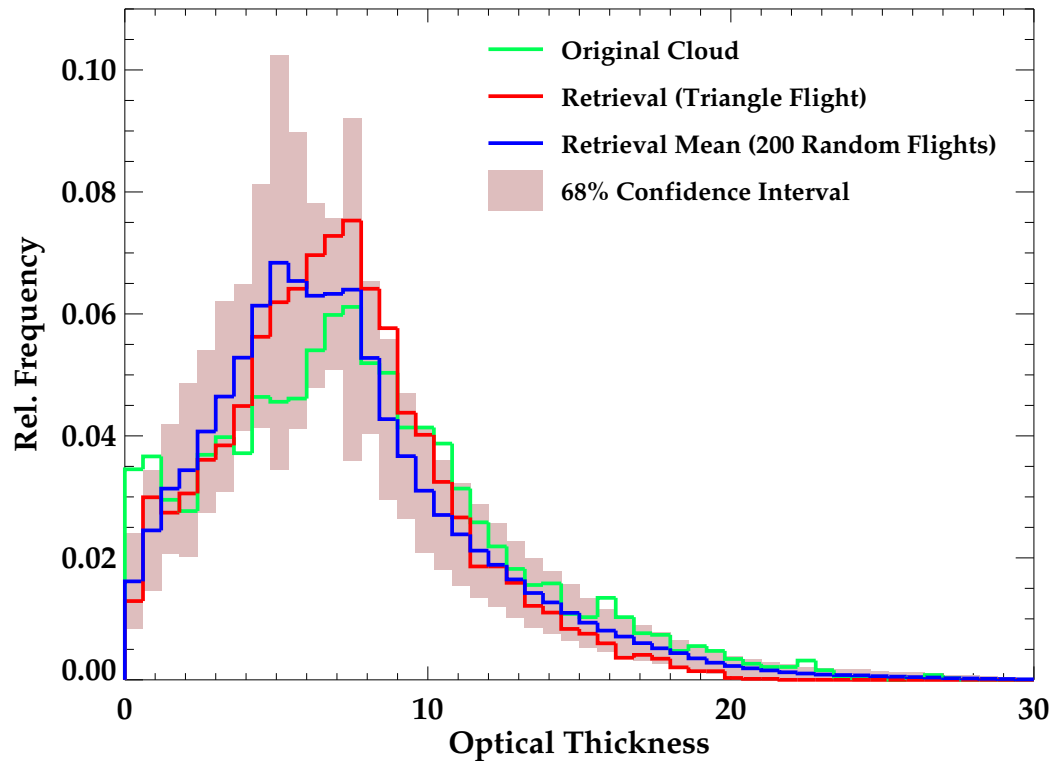


Fig. 3. Frequency of optical thicknesses for the original cloud field (green), the retrieval from triangular flight (red), and the mean of 200 retrievals (blue). The shaded area marks the 68% confidence interval.

[Title Page](#)[Abstract](#)[Introduction](#)[Conclusions](#)[References](#)[Tables](#)[Figures](#)[◀](#)[▶](#)[◀](#)[▶](#)[Back](#)[Close](#)[Full Screen / Esc](#)[Print Version](#)[Interactive Discussion](#)

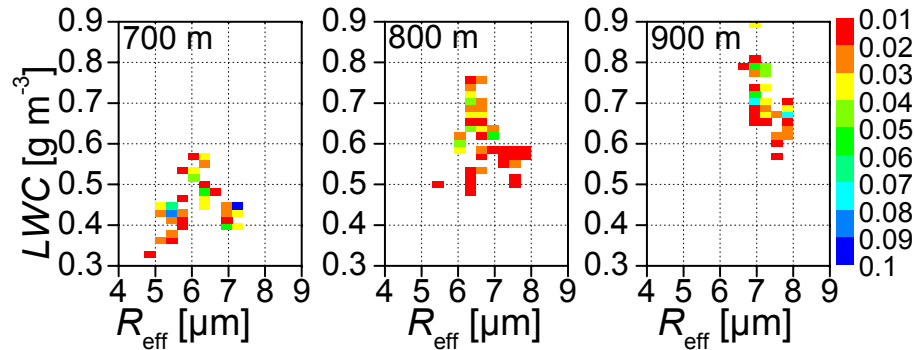
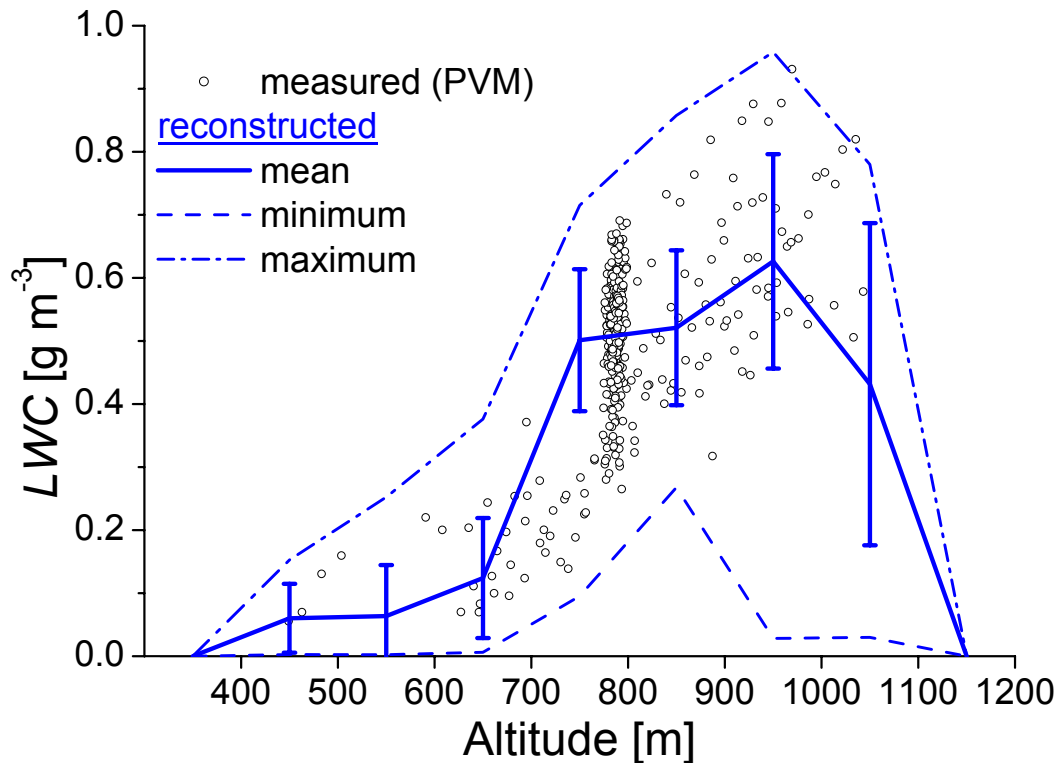
Retrieving cloud structure from airborne measurementsR. Scheirer and
S. Schmidt

Fig. 4. Two-dimensional “PDF” of the measured liquid water content and the effective drop radius at three altitudes.

[Title Page](#)[Abstract](#)[Introduction](#)[Conclusions](#)[References](#)[Tables](#)[Figures](#)[◀](#)[▶](#)[◀](#)[▶](#)[Back](#)[Close](#)[Full Screen / Esc](#)[Print Version](#)[Interactive Discussion](#)

Retrieving cloud structure from airborne measurementsR. Scheirer and
S. Schmidt**Fig. 5.** Measured and reconstructed *LWC* profile.[Title Page](#)[Abstract](#)[Introduction](#)[Conclusions](#)[References](#)[Tables](#)[Figures](#)[◀](#)[▶](#)[◀](#)[▶](#)[Back](#)[Close](#)[Full Screen / Esc](#)[Print Version](#)[Interactive Discussion](#)

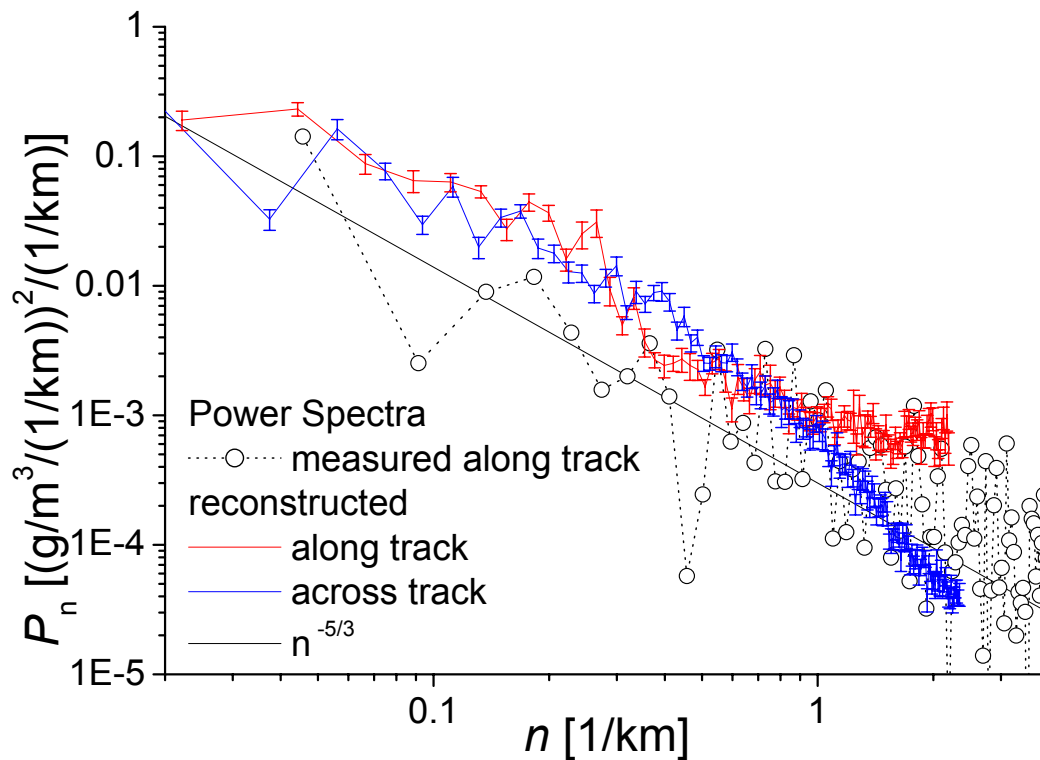
Retrieving cloud
structure from
airborne
measurementsR. Scheirer and
S. Schmidt

Fig. 6. Measured and reconstructed Power Spectrum of the LWC.

[Title Page](#)[Abstract](#)[Introduction](#)[Conclusions](#)[References](#)[Tables](#)[Figures](#)[◀](#)[▶](#)[◀](#)[▶](#)[Back](#)[Close](#)[Full Screen / Esc](#)[Print Version](#)[Interactive Discussion](#)